Pairing, π-bonding, and the role of nonlocality in a dense lithium monolayer

A. Bergara,* J. B. Neaton, and N. W. Ashcroft
Laboratory of Atomic and Solid State Physics and the Cornell Center for Materials Research, Cornell University, Ithaca, New York 14853-2501
(Received 22 March 2000)

Results of self-consistent *ab initio* all-electron calculations of a lithium monolayer are presented. Upon increase in mean density, the electronic structure of the monolayer is found to deviate significantly from nearly free electronlike behavior: instead of growing with compression, the width of lowest subband actually diminishes. The resulting band structure exhibits a π-bonding character, and it is found that this feature cannot be modeled with a local pseudopotential. Similar to the case in three dimensions, the monatomic monolayer is also found to be unstable to pairing at $r_s = 1.96$.

I. INTRODUCTION

In their most dilute phases, the group-I elements (the alkalis) exist as weakly interacting atomic and molecular vapors. As the density increases, the atomic and molecular wave functions overlap, broadening the formerly discrete electronic levels into bands. For all group-I elements except hydrogen, the ensuing intermolecular interactions result in dissociation and the formation under ambient conditions of a monatomic metallic liquid or solid. Because of their monovalency and high conductivity, the light alkali metals have long been considered prototypical *simple metals*. Indeed it is commonly anticipated that the electronic structure of the alkalis should become even simpler under compression.[1] However, when lithium and sodium are compressed, significant deviations from this elementary picture have been recently predicted. First-principles calculations show diminishing coordination with increasing pressure and nearly insulating electronic properties close to fourfold compression in lithium.[2] Experiments performed with diamond-anvil cells have measured changes in optical properties in lithium which are consistent with this prediction;[3,4] a recent shock experiment reports a negative temperature derivative of the dc conductivity above 60 GPa,[5] indicative of activated or semiconducting behavior for lithium at these elevated pressures and temperatures.

Many of these important differences in physical properties may be expected to persist as the dimensionality of the system is decreased, and this has prompted the present study of Li monolayers. Although the monolayer (ML) consists of three-dimensional atoms, their associated electrons are mainly confined within an atomic plane. Atomic monolayers have been studied in the past to analyze the insulator-metal transition at lower dimensions.[6] With the advent of new techniques in atomic manipulation using scanning tunneling microscopy (STM),[7] it is now possible to study the effects of dimensionality by experiment. In addition, it may be possible to study MLs of variable density by deposition on inert substrates and even under compression through implementation of a ''sandwich'' geometry.

An evident consequence of the planar confinement is the lower coordination as compared to the bulk, and the expectation is that atoms in the ML should then be less strongly bound. But this change in the coordination number may also have a profound effect on the nature of the chemical bond between the atoms. For example, diamond possesses covalent tetrahedral bonds, while graphite is a layered π-bonded material. Different orbital hybridizations and occupancies at low dimensions can lead to interesting variations in both electronic and structural properties.

In what follows, we present results of self-consistent *ab initio* all-electron calculations of a single lithium ML, treating the ions as static. Because of the remarkable changes in electronic and structural properties already occurring in three dimensions, a first-principles study of a lithium ML under compressive strain is also expected to lead to a better understanding of the bulk system. In addition, it can assist more generally in providing further insight into the behavior of electrons in low-dimensional systems. Section II describes the theoretical and computational methods that we have used in this study. In Sec. III we present our results. In Sec. IV we use a nonlocal pseudopotential model to explain the major novel features observed at high densities. Finally, conclusions are presented in Sec. V.

II. METHODOLOGY

To investigate the electronic properties of a ML from first principles, we employ density functional theory (DFT) within the local density approximation[8] (LDA) and with an assessment of gradient corrections (see below). In many implementations of DFT using plane-wave basis sets, the core electrons are integrated out of the problem and incorporated, with the nuclei, into ionic cores. The resulting interaction between the valence electrons and ions, or *pseudopotential* (generally nonlocal), simplifies the calculation by reducing the number of required basis functions. While this approach is successful in modeling solids at their normal stabilizing densities, it requires increasing scrutiny as the atomic spacing is reduced and the cores overlap. All-electron calculations, which fully treat the core electrons, are then better suited for predicting the behavior of solids under significant compression. But because of the divergence of the Coulomb potential at the nucleus, many plane waves are necessary to converge both total energies and, most important to our application, *total energy differences*. The large plane-

wave cutoffs are impractical, and here we make use of a newly developed method, the projector augmented-wave (PAW) method.[9] All-electron PAW potentials, treating both the 1*s* and 2*s* states as valence, have had success reproducing previous LDA work on bulk and molecular lithium;[10] they have also been used recently for predicting new phases of bulk lithium at high pressure.[2]

In what follows we have used the Vienna *ab initio* simulations package[11] (VASP) to calculate total energies and electronic properties at several densities. Because core overlap may affect the accuracy of calculations for small interatomic spacings, the all-electron PAW, calculations are used for atomic densities[12] corresponding to $r_s < 2.5$. To obtain the equilibrium properties of the monolayer, total energies were evaluated with a Vanderbilt ultrasoft pseudopotential[13,14] (US-PP) at lower densities ($r_s > 2.5$). Although more complex structures can be envisaged, we have selected three competitive lattices for study: a square (sq), a hexagonal (hex), and a paired-square (p-sq) structure. The paired-square structure consists of a square cell with a two-atom basis (one atom at the corner and the other near the center). The supercell containing the lithium monolayer incorporates ten equivalent layers of vacuum (absence of atoms) in order to minimize any Coulomb and exchange interaction between monolayers. The lattice spacing was systematically reduced to simulate the effects of compression, and the total energy and electronic properties were subsequently determined as a function of area. The ions were relaxed into their equilibrium positions using forces calculated from the Hellmann-Feynman theorem. Throughout the calculations the system has been confined to a plane (i.e., no buckling out of the plane is presently permitted[15]). The confined ions interact at long range via the full three-dimensional (3D) Coulomb potential: both field lines and electronic charge density are therefore allowed to extend out of the plane.

III. RESULTS

At an equilibrium density of $r_s = 3.02$ (a unit cell area of $A_0 = 28.75$ a.u.^{2}), the ML considerably favors hex over the sq structure by 63 meV/ion (Fig. 2). The nearest-neighbor distance (5.80 a.u.) is just 4% larger than the interatomic distance of bulk bcc lithium (5.52 a.u.), indicating, as suggested above, that the ML has weaker binding because of the reduced coordination. Since lithium atoms have open-shell $2s^1$ electronic configurations, the lithium molecule can be quite strongly bound, and the calculated bond length of the Li_2 molecule (5.12 a.u. within the LDA) is thus smaller than the nearest-neighbor distance of both the bulk and ML. In Fig. 1 the corresponding band structure for the hex ML at equilibrium is shown. As expected, the occupied lowest band has an *s*-like character and an essentially nearly free electronlike dispersion, although the gap at *M* is comparable to the bandwidth ($\sim$3 eV), as is the case in three dimensions. The bottom of the next-highest subband is found to be 0.34 eV *above* the Fermi energy (E_F), and these states have a p_z symmetry: i.e., their charge distribution is perpendicular to the plane and therefore characteristic of π-bonding. In contrast to the known electronic structure of the heavier

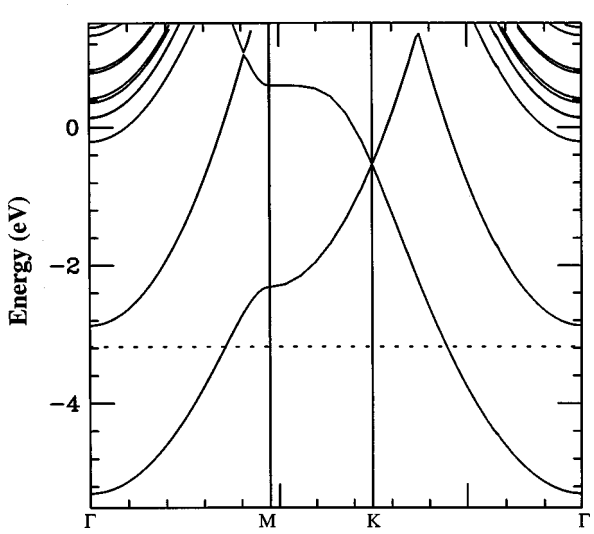

FIG. 1. Band structure of a hexagonal lithium monolayer at equilibrium ($r_s = 3.02$). As expected for lithium, only the lowest ($2s$) band is occupied. The Fermi energy is represented by the dotted line. Although the occupied band has essentially free-electron-like dispersion, the gap observed at *M* is notably large.

alkalis,[16] the *d*-like states remain well above E_F and there is little *s-d* hybridization.

In Fig. 2 we have plotted the calculated enthalpies for the three structures considered, and we observe two structural phase transitions as the density of the monolayer increases. We find that at $r_s = 1.96$ ($A/A_0 = 0.42$) the lithium ML becomes unstable to *pairing*, exactly as in three dimensions. In the p-sq structure the dimer is oriented along the diagonal of the square, initially with an intra-atomic distance of 2.78 a.u., which decreases to 2.00 a.u. at $r_s = 1.4$. As the density increases to $r_s = 1.34$ ($A/A_0 = 0.20$), the p-sq structure gives way to the relatively open sq structure. This is stable to the highest densities considered ($r_s = 1$) and becomes even more stable as the density increases despite the (Madelung) energetic cost for four-fold coordination (as opposed to higher packing in the hex structure). The transition from a paired structure to an open structure (rather than to a close-packed arrangement) closely parallels previous predictions for dense lithium and hydrogen[17] in 3D, where the paired *Cmca* phase was found for both cases to be unstable to an eventual Cs-IV structure. The effects of gradient corrections[18] are found to be minimal: they do not shift the transition densities, but they do result in a slightly larger dimer length at each volume than that calculated within the LDA. Calculations within the local spin-density approximation (LSDA) do not change the total energies at densities considered in this study.

As in the 3D case, an increase in density has an unexpected effect on the electronic structure, and we find that the lithium ML becomes progressively *less* free-electron-like. In Fig. 3 we show the band structure of a lithium ML at $r_s = 2$ near the density at which the pairing instability occurs. Despite the elevated density, the bandwidth of the first subband is nearly the same as at $r_s = 3.02$ (Fig. 1), although the gap at *M* has nearly tripled in size. As the monolayer is compressed further, the energy gap at Γ decreases and, crucially, the upper p_z subband begins to overlap the *s* subband. In fact, near $r_s = 2.1$, the upper subband is *occupied* and as a consequence the valence electrons now assume a distinct

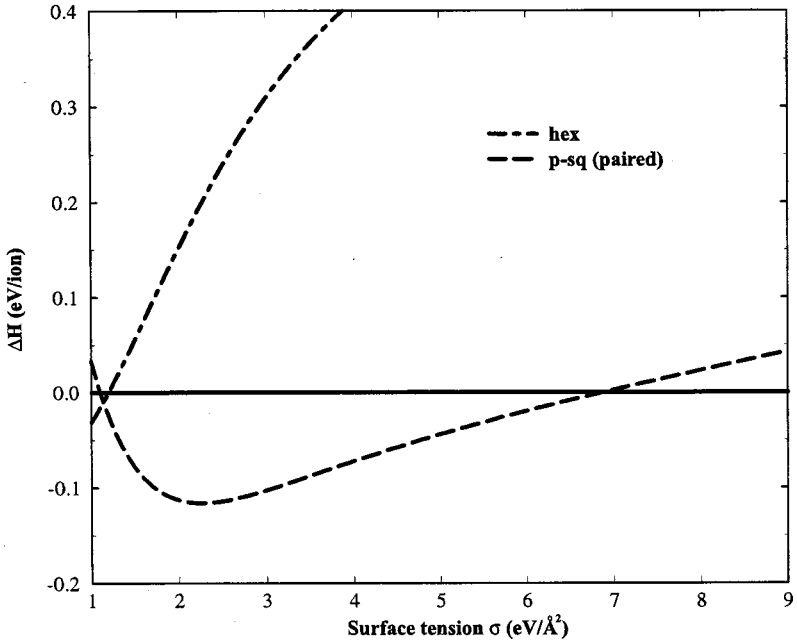

FIG. 2. Enthalpy ($H=E+\sigma A$) as a function of intralayer *surface tension* $\sigma=-dE/dA$ for competitive structures of lithium; all enthalpies are referenced to the square structure ($\Delta H=H-H_{sq}$). The total energies are well fit to $E(A)=a_1+a_2A^{-1/2}+a_3A^{-1}+a_4A^{1/2}+a_5A$. Our calculations with the all-electron PAW potentials (having core radii of 1.1 a.u. required an 80-Ry cutoff and k-point meshes of $20\times20\times2$ for a relative error in the total energy of 1 meV/atom. Calculations with a single-valence US-PP (incorporating the $1s$ states into the core) confirm most features (including the pairing) predicted with the all-electron potential, even at densities in which there is appreciable core overlap between neighbors. However, the differences in energy observed between both methods increases at high densities ($r_s<2$), illustrating the important role of the core electrons in determining the total energy at these densities.

π-bonding character. New pathways for conduction therefore open.

The electronic structure continues to differ from nearly free electronlike behavior at densities near and above the pairing instability. Figure 4 shows the energy band dispersion for the p-sq structure at $r_s=1.65$. The $2s$ subband actually *flattens* and the band gap at Γ is *negative* (the p_z subband has now progressed below the $2s$ subband), resulting in an increase in the number of conducting electrons with π-bonding character and continuing the trend observed in the monatomic case. Although the presence of two electrons per unit cell satisfies the necessary condition for insulating behavior, the lithium ML remains metallic because of the overlap between the first two *subbands* (an interesting difference from 3D). For larger densities the bottom of the π band drops with respect to the $2s$ band and, contrary to free-electron-like (k^2-type) behavior, the minimum point in the band is at the edge of the Brillouin zone. The flat dispersion at the zone boundary results in van Hove singularities near the Fermi energy, markedly increasing the density of states there. These two features are not unexpected: at sufficiently high densities the gap between the $1s$ and $2s$ bands will inevitably close.

As in three dimensions, the growing pseudopotential (as evidenced by the increased gap at M in Fig. 3) results in an electronic configuration unstable to a Peierls-type symmetry breaking, which will lower the kinetic energy. Indeed, we observe that the kinetic energy of the electrons in the paired structure compensates the expected increases in Madelung and Hartree energies above $r_s=1.96$. The growing pseudopotential can be interpreted as the result of the exclusionary

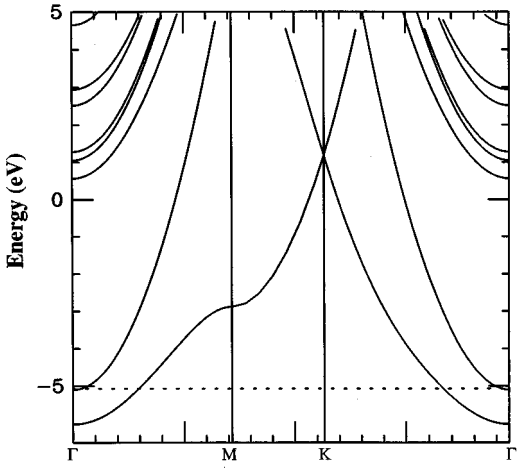

FIG. 3. Band structure of a hexagonal lithium ML at $r_s=2.0$ (near the pairing instability). The bandwidth of the first subband has decreased with respect to the substantial gap at M compared with the bands in Fig. 1. The second band, having π-bonding character, is also partially occupied at this density.

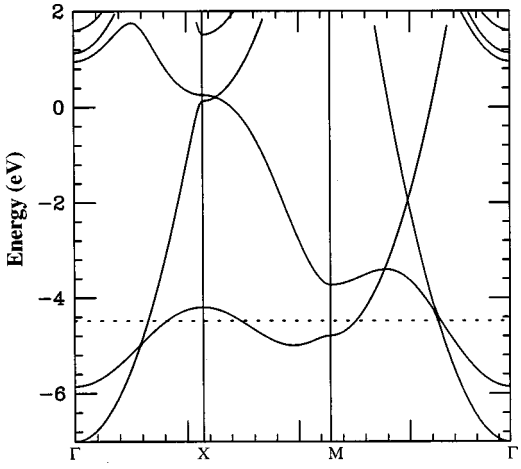

FIG. 4. Band structure of the paired-square lithium ML at $r_s=1.65$. The difference between lowest energy levels at Γ changes as the p_z subband drops below the s subband, a result of the increasingly nonlocal character of the electron-ion interaction with increasing density. The number of conducting electrons with π-bonding character increases with density, significantly changing the electronic properties of the monolayer.

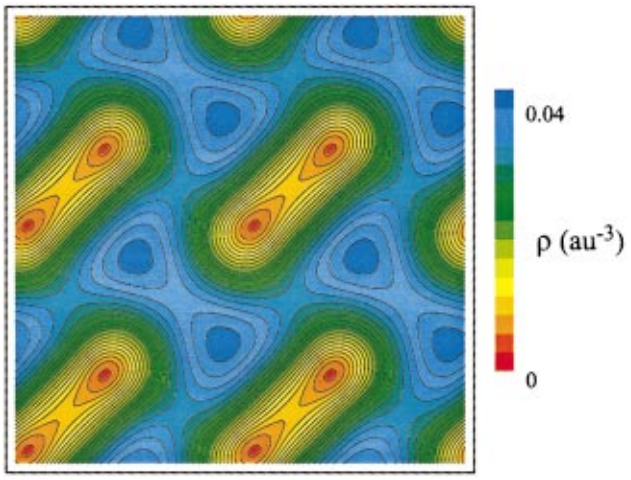

FIG. 5. (Color) LDA valence charge density of a paired-square lithium monolayer at $r_s=1.65$. The ions are centered in the red regions, and the valence charge density (blue areas) prefers regions *away* from the pairs, accumulating in both the interstitial in-plane regions and extending further into the z direction. It is lowest near the nuclei and along the dimer.

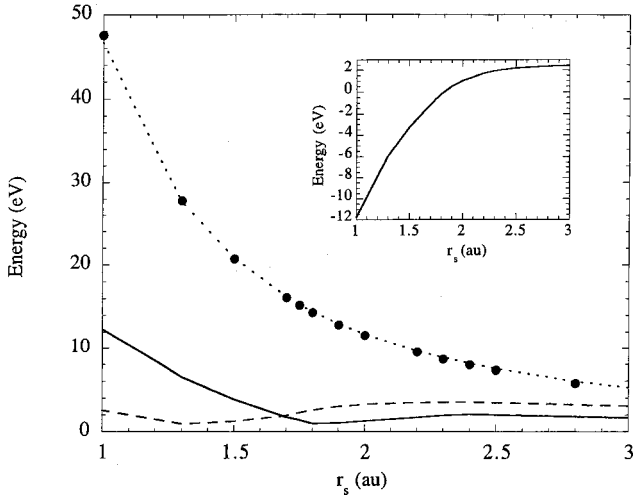

FIG. 6. Occupied bandwidth (solid line), p_z bandwidth (black dots), and s bandwidth (dashed line) at the M point in the BZ of a hexagonal lithium ML plotted as a function of density as calculated within the LDA. The p_z bandwidth at M is well fit by $47/r_s^2$ eV (dotted line), where $49/r_s^2$ is the bandwidth for the strictly two-dimensional free-electron gas (the $2s$ bandwidth is nearly independent of density). In the inset, the solid line represents the energy difference between the first two levels at the Γ point, which becomes *negative* at $r_s=1.8$ as the p_z subband drops below the s subband.

effects of the core electrons, which overlap under pressure and force the valence electrons into the interstitial regions. This is reflected by the electronic charge density distribution which is shown in Fig. 5 for the p-sq structure of the lithium monolayer at $r_s=1.65$. Notice that the valence electron density is *highest* within the interstitial regions: in contrast to the dilute molecular phase in which the density is highest between pairs, the charge density is rejected from that region (as in 3D). Because of the π-like nature of the band structure, there is also an excess of charge decaying out of the plane. Both of these features result from the Pauli principle and orthogonalization: the valence electrons energetically prefer to reside outside the cores and regions of large core overlap, lowering its kinetic energy.

IV. DISCUSSION

The nearly free electron model normally assumes that the electron-ion interaction H_{ei} is weak and *local*. If the monolayer is nearly free electronlike, the band gap at the Brillouin zone (BZ) boundary, proportional to the strength of the electron-ion coupling, should be small; further, if the electron-ion interaction is completely *local*, the kinetic energy should dominate and the bandwidth should *increase* with density relative to the gaps at the boundaries. To illustrate, consider the scaling properties of the matrix elements of a purely local empty-core pseudopotential,[19] i.e.,

$$V(G)=\frac{-4\pi Ze^2}{\Omega}\frac{1}{G^2}\cos GR_c, \tag{1}$$

where Z is the nuclear charge, Ω is the volume of the unit cell, and R_c represents the core radius. The density dependence of the gap at the BZ boundary $[\propto 2|V(G)|]$ for this pseudopotential is $1/r_s$, and, on the other hand, the free-electron Fermi energy E_F^0 scales as $1/r_s^2$. Therefore, the ratio between the band gap and the Fermi energy is *linear* in the lattice constant $[|V(G)|/E_F^0 \propto r_s]$ and the BZ boundary gap should be expected to *close* as the lattice constant decreases. In our LDA calculations summarized in Fig. 6, however, it is clear that the gap at the BZ boundary *grows* with increasing density (leading to the pairing instability) and the $2s$ bandwidth *diminishes*. In fact, the p_z subband drops below the Fermi energy near $r_s=2.1$ and then below the $2s$ subband at $r_s=1.8$. As Fig. 6 attests, the p_z bandwidth fits quite well to $1/r_s^2$, indicating its nearly free electron behavior. Conversely, the $2s$ bandwidth decreases slightly with density, and this flattening behavior cannot be described within nearly free electron physics.

A local pseudopotential, which leads to a linear density scaling of the strength of H_{ei} with respect to the bandwidth, treats the electron-ion interaction without regard to the symmetry of the Bloch valence wave function. However, as is shown in Fig. 6, we have observed quite different density scaling properties depending on the angular momentum character of the wave function. Therefore, we consider the following *nonlocal* pseudopotential model:[20]

$$H_{ei}=V(r)+\sum_{c,\mathbf{R}}(\epsilon-E_c)|\psi_{c,\mathbf{R}}\rangle\langle\psi_{c,\mathbf{R}}|, \tag{2}$$

where $|\psi_c\rangle$ is a core state and $V(r)$ is a completely local potential consisting of the bare Coulomb interaction $-3/r$ and a screening term arising from the Hartree repulsion of the core states ($1s$ in this case). For lithium, the repulsive component of the pseudopotential in Eq. (2) *only* projects out the s character of the wave function. On the other hand, the p character will sample the full nuclear potential $(-3/r)$ as there is no effect from orthogonalization. Therefore, for the p- (and higher l-) projected components of the Bloch wave functions there will be a stronger potential at each site and an

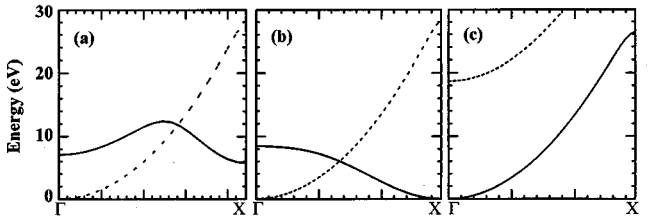

FIG. 7. The lowest two valence bands for the square lithium monolayer at $r_s=1.2$ calculated from (a) first principles using the PAW technique, (b) the *non local* pseudopotential specified in Eq. (2), and (c) the *local* pseudopotential of Eq. (1). Note the significant differences between both approximations (b) and (c); only the *nonlocal* model (b) can reproduce the high-density characteristics of the monolayer determined with the LDA: the p_z subband (dashed line) dropping below the $2s$ subband (solid line) at Γ and the flattening of the $2s$ band. The p_z bandwith obtained with both models is very similar ($\sim$30 eV). Both approximations include only the electron-ion interaction, allowing us to attribute the observed drastic changes in electronic properties to nonlocality. We used 243 plane waves (30-Ry cutoff) for both models with 10 Å of vacuum between planes. For the *local* pseudopotential we have considered $R_c=0.56$ Å (as in Ref. 21) for the core radius of lithium. In the *nonlocal* model,[22] we use a hydrogenic wave function $\psi(\mathbf{r})=(Z^3/\pi)^{1/2}e^{-Zr}$ as the core state, even at densities predicted (by our LDA calculations) to have significant $1s$ (core) bandwidth. Both $\Delta E=\epsilon-E_c$ and Z were adjusted to fit our calculated LDA band structures, and we found that $\Delta E=2.4$ Ry and $Z=2.8$ reproduced the calculated band structures at equilibrium densities.

energy benefit for electronic charge with this symmetry. This accounts for the difference in scaling between the p_z bandwidth and $2s$ bandwidth: interacting via a purely local potential, the kinetic energy (bandwidth) of the p_z charge will scale with the potential as originally assumed. As can be seen in Fig. 7, band structures calculated with a nonlocal pseudopotential reproduce the high-density characteristics of the monolayer determined with the LDA: the p_z subband drops below the $2s$ subband at Γ, and the $2s$ band flattens. The importance of *nonlocal* effects has already been mentioned before[23] in the context of bulk lithium at high densities, in which the p band was observed to grow faster than the s band (ultimately resulting in the s-to-p transition). Likewise in that case, core overlap reduces the amount of space available to the valence electrons at higher densities, increasing the probability that they occupy the interstitial regions. The overall energy is then lower in states having p-like symmetry because of their stronger attraction to the nucleus.

V. CONCLUSIONS

We have presented the results of self-consistent *ab initio* all-electron calculations of a lithium monolayer as a function of the interatomic spacing. These calculations show that under compression the lithium monolayer becomes less free-electron-like with a remarkable flattening of the first subband and an associated large gap at the Brillouin zone boundary, both of which can only be understood in terms of a nonlocal electron-ion interaction. As the interatomic distance is decreased, we have also observed gap closure at Γ. As a consequence, the π-bonding character subband is filled, opening a new path for conduction. The departure from nearly free electron behavior also leads to structural phase transitions, and monoatomic lithium monolayers are predicted to become unstable to pairing at higher densities. The observed features are not unique to lithium, and preliminary calculations indicate that similar transitions also occur in sodium and beryllium, but at considerably higher compressions. In principle, MLs could also be formed at progressively *lower* density, and calculations indicate that near $r_s=4.1$, the lithium monolayer becomes unstable to the formations of dimers *preceding* the metal-insulator transition. Extensions of this work to consider possible structures with more than one pair per unit cell and also allowing the atoms to buckle out of the plane would be of considerable interest in order to analyze possible many-body consequences, e.g., the formation of charge density waves and possibility of superconductivity,[15] both at higher densities and lower.

ACKNOWLEDGMENTS

This work was supported by the National Science Foundation (DMR-9988576). This work made use of the Cornell Center for Materials Research Shared Experimental Facilities, supported through the National Science Foundation Materials Research Science and Engineering Centers program (DMR-9632275). A.B. would like to acknowledge financial support from the Spanish Ministerio de Educatión y Cultura under Fulbright Grant No. FU-99-30656084.

*Permanent address: Materia Kondentsatuaren Fisika Saila, Zientzia Fakultatea, Euskal Herriko Unibertsìtatea, 644 Posta Kutxatila, 48080 Bilbo, Spain.

[1] The idea originated with J. D. Bernal. See E. Wigner and H. B. Huntington, J. Chem. Phys. **3**, 764 (1935).

[2] J. B. Neaton and N. W. Ashcroft, Nature (London) **400**, 141 (1999).

[3] A. Ruoff and Y. Mori (unpublished).

[4] V. V. Struzhkin, R. J. Hemley, and H. K. Mao (unpublished).

[5] V. E. Fortov, V. V. Yakushev, K. L. Kagen, I. V. Lomonosov, V. I. Postnov, and T. I. Yaksusheva, Pis'ma Zh. Eksp. Teor. Fiz. [JETP Lett. **70**, 628 (1999)].

[6] H. J. F. Jansen, A. J. Freeman, M. Weinert, and E. Wimmer, Phys. Rev. B **28**, 593 (1983); E. Wimmer J. Phys. F: Met. Phys. **13**, 2313 (1983); T. Yamada and Y. Yamamoto, Phys. Rev. B **54**, 1902 (1996).

[7] Some examples are D. M. Eigler and E. K. Schweizer, Nature (London) **344**, 524 (1990); H. Uchida, D. H. Huang, F. Grey, and M. Aono, Phys. Rev. Lett. **70**, 2040 (1993); C. T. Salling and M. G. Lagally, Science **265**, 502 (1994).

[8] P. Hohenberg and W. Kohn, Phys. Rev. B **136**, B864 (1964); W. Kohn and L. J. Sham, Phys. Rev. A **140**, A1133 (1965).

[9] P. E. Blöchl, Phys. Rev. B **50**, 17 953 (1994).

[10] G. Kresse and D. Joubert, Phys. Rev. B **59**, 1758 (1999).

[11] G. Kresse and J. Hafner, Phys. Rev. B **47**, RC558 (1993); G. Kresse and J. Furthmüller, *ibid.* **54**, 11 169 (1996).

[12] Here we have defined the two-dimensional linear density parameter r_s by the relation $A/N=\pi(r_s a_0)^2$ for N nuclei in a monolayer of area A, with a_0 being the Bohr radius.

[13] D. Vanderbilt, Phys. Rev. B **41**, 7892 (1990).

[14] For densities less than $r_s=2.5$, the US-PPs produced results

equivalent to the all-electron calculations. This indicates that the core electrons are important for $r_s > 2.5$, but can be ignored at lower densities. The lithium US-PP was provided by G. Kresse. See G. Kresse and J. Hafner, J. Phys.: Condens. Matter **6**, 8245 (1994).

[15] A. Bergara, J. B. Neaton, and N. W. Ashcroft (unpublished).

[16] S. G. Louie and M. L. Cohen, Phys. Rev. B **10**, 3237 (1974).

[17] K. A. Johnson and N. W. Ashcroft, Nature (London) **403**, 632 (2000).

[18] J. P. Perdew, J. A. Chevary, S. H. Vosko, K. A. Jackson, M. R. Pederson, D. J. Singh, and C. Fiolhais, Phys. Rev. B **46**, 6671 (1992).

[19] N. W. Ashcroft, Phys. Lett. **23**, 48 (1966).

[20] J. C. Phillips and L. Kleinman, Phys. Rev. **116**, 287 (1959); M. L. Cohen and V. Heine, Solid State Phys. **24**, 37 (1970).

[21] N. W. Ashcroft and D. C. Langreth, Phys. Rev. **155**, 682 (1967).

[22] J. B. Neaton, Ph.D. Thesis, Cornell University (2000).

[23] J. C. Boettger and S. B. Trickey, Phys. Rev. B **32**, 3391 (1985); W. G. Zittel, J. Meyer-ter-Vehn, J. C. Boettger, and S. B. Trickey, J. Phys. F: Met. Phys. **15**, L247 (1985).